Feasibility analysis on transient speed of sound investigations using laser-induced thermal acoustics in evaporating droplets.

Christoph Steinhausen[1,*], Valerie Gerber[1], Andreas Preusche[2], Andreas Dreizler[2], Bernhard Weigand[1], Grazia Lamanna[1]
1: Institute of Aerospace Thermodynamics, University of Stuttgart, Germany
2: Institute Reactive Flows and Diagnostics, Technical University of Darmstadt, Germany
* Correspondent author: christoph.steinhausen@itlr.uni-stuttgart.de

Keywords: LITA, LIGS, Evaporation, Near-Critical

ABSTRACT

The development of combustion processes to achieve higher efficiencies has led to a continuous increase in operating pressures that exceed the critical point of the injected fluids. Especially for supercritical atmospheric conditions with respect to the injected fluid, the fundamental physics of the occurring mixing and evaporation processes are not fully understood. In particular, quantitative data for the validation of numerical simulations as well as analytical models remain sparse. Laser-induced thermal acoustic (LITA), also known as laser-induced grating spectroscopy (LIGS), is a seedless, non-intrusive measurement technique capable of detecting speed of sound data as well as acoustic attenuation within these mixing processes. Until now, the feasibility of time-resolved LITA measurements in complex fluid dynamic processes has not been proven. Therefore, a feasibility analysis on transient speed of sound investigations using laser-induced thermal acoustics in evaporating droplets has been conducted. LITA has hereby been applied in the wake of a free-falling acetone droplet evaporating in a nitrogen atmosphere at nearcritical conditions. To the authors' best knowledge, this is the first-time transient LITA measurements investigating macroscopic fluid phenomena, such as fluid injection and evaporation processes, have been conducted. The evaporation of the droplet has been simultaneously visualised using shadowgraphy, whereas time-resolved speed of sound data have been directly detected by a high-speed LITA system with a high-repetition rate excitation laser source. The measurement position is hereby located at a fixed position in the wake of the droplet. The speed of sound data indicate a higher concentration of acetone as well as temperatures below the operating conditions in the wake of the droplet. This indicates a classical two-phase evaporation process, resulting in an evaporative cooling of the droplet and the subsequent mixing process in its wake. Moreover, the experimental results prove the feasibility of time resolved laser-induced thermal acoustics measurements in macroscopic fluid phenomena.

1. Motivation

Understanding droplet evaporation processes has increasingly become important for achieving a stable and efficient combustion. As the entropy production is reciprocally dependent on the density, higher pressures lead to a reduction in entropy production and, hence, a more efficient

process, combustion pressures have increased in the last decade to the point that they exceed the critical values of the injected fluids. Particularly for supercritical pressures with respect to the injected fluid, mixing and evaporation processes are not fully understood yet. As is evident by recent publications by (Baab, et al., 2016), (Baab, et al., 2018), (Crua, et al., 2017), (Falgout, et al., 2016), (Gerber, et al., 2021), (Müller, et al., 2016), and (Preusche, et al., 2020) in the last decade, near- to supercritical evaporation and mixing processes have received increased attention. However, quantitative data for validation of numerical simulation remain sparse and are a research objective with increasing interest, see (Bork, et al., 2017), (Gerber, et al., 2021), (Lamanna, et al., 2018), (Preusche, et al., 2020), and (Steinhausen, et al., 2019).

Laser-induced thermal acoustics (LITA) has been used by (Stampanoni-Panariello, et al., 2005) for gas-phase diagnostics, such as thermometry, velocimetry, and concentration measurements. By analysing the grating lifetime (Willman, et al., 2021) have determined the pressure. The first time-resolved thermometry investigations using LITA under static cell conditions have been conducted by (Förster, et al., 2017). The feasibility to apply LITA for investigating macroscopic fluid phenomena such as high-pressure jet injection has been proved by (Baab, et al., 2018). The authors measured the speed of sound of the mixture along the radial as well as the lateral axis of the jet.

The objective of this work is to present the feasibility of time-resolved measurements using laser-induced thermal acoustics under complex flow conditions, such as in the wake of an evaporating droplet. To the authors' best knowledge this is the first-time transient LITA measurements investigating macroscopic fluid phenomena, such as fluid injection processes, are conducted.

2. Theoretical background

By analysing the frequency spectrum of the LITA signal, the speed of sound c_s can be directly extracted using equation (1).

$$c_s = \frac{\nu \Lambda}{j} \qquad (1)$$

The dominating frequency ν of the LITA signal is hereby calculated using a direct Fourier transformation (DFT) together with a von Hann window and a bandpass filter. The constant j indicates the resonant fluid behaviour with respect to the wavelength of the excitation beams. In case of a non-resonant fluid $j = 2$ is applied, whereas in case of resonant fluid behaviour $j = 1$,

referred by (Hemmerling & Kozlov, 1999). The grid spacing of the optical interference pattern is denoted with Λ and is a calibration parameter for the optical setup.

Using the extended approach for the time-based LITA evaluation methodology proposed by (Steinhausen, et al., 2021), it is possible to extract macroscopic fluid properties from the shape of the LITA signal. The physical and mathematical derivation of this time-based approach was developed by both (Cummings, et al., 1995) and (Schlamp, et al., 1999).

Mathematically, the detected LITA signal $\eta(t)$ depends on three fluid properties, namely the speed of sound c_s, the thermal diffusivity D_{th} as well as the acoustic damping rate Γ. Additionally, the following dependencies can be observed

$$\eta(t) = \frac{I_{exc}}{I_{int}} \propto f(D_T, \Gamma, c_s, t_0, \bar{\eta}, q, \sigma, \omega, t), \qquad (2)$$

where I_{exc} and I_{int} are the intensities of the excitation and the interrogation beam, respectively. The Gaussian half width of the excitation beams are denoted by ω, whereas the Gaussian half width of the interrogation beam is expressed by σ. Both beam sizes are calibration parameters. The time of the laser pulse t_0 and the beam misalignment $\bar{\eta}$ are fitting constants. Note, that the magnitude of the grating wave vector q depends on the grid spacing Λ. The latter is a function of the crossing angle Θ of the excitation beams and the wavelength of the excitation pulse λ_{exc}, see equation (3) in (Still, 2009) and (4) in (Hemmerling & Kozlov, 1999).

$$q = \frac{2\pi}{\Lambda} \qquad (3)$$

$$\Lambda = \frac{\lambda_{exc}}{2\sin\left(\frac{\Theta}{2}\right)} \qquad (4)$$

Applying a Levenberg–Marquardt curve fitting algorithm based on equation (2) to the LITA signal an estimation of the thermodynamic variables c_s, D_{th} and Γ is possible. For mixing processes, such as high-pressure turbulent jet mixing or the dense fluid mixing in the wake of an evaporating droplet in the vicinity of the critical point, these thermodynamic properties can be used to derive the mixing state, as previously proposed by (Steinhausen, et al., 2021). However, a model for the acoustic damping rate for binary mixtures as well as pure fluids at high pressure conditions is necessary. Based on a literature review such models are sparse. Due to the short residence time, for the presented investigation we propose an adiabatic mixing model, which was successfully

applied for similar conditions by (Bork, et al., 2017) and (Preusche, et al., 2020) as well as theoretically argued by (Lamanna, et al., 2020). As shown in (Preusche, et al., 2020), the applicability of the adiabatic mixing assumption is justified and corroborated by direct measurements of the droplet temperature by laser-induced fluorescence and phosphorescence. Using the NIST Database by (Lemmon, et al., 2018) to compute the speed of sound of the mixture $c_{s,mix}$, the dependencies are as follows

$$c_{s,mix}(p_{ch}, T_{mix}, x_{Fl,mix}) = c_{s,LITA}. \qquad (5)$$

Due to the controlled environment, the pressure in the measurement chamber p_{ch} is known. Since the adiabatic mixing assumption connects the mixing temperature T_{mix} and the concentration of the mixture $x_{Fl,mix}$, we are able to determine the mixture state using the measured speed of sound data.

3. Optical setup

Laser-induced thermal acoustics (LITA) utilises the interactions of matter with an optical interference pattern to detect independently and simultaneously speed of sound, acoustic damping rate as well as thermal diffusivity. The interference pattern is created by two short-pulsed excitation beams generated by a high frequency pulsed Nd:YAG laser (Edgewave INNOSLAB) with a wavelength of $\lambda_{exc} = 1064$ nm, an operating frequency of 10 kHz, a laser pulse length of $\tau = 8.8$ ns and a 53 GHz linewidth. A third input wave from a continuous wave DPSS laser (Coherent Verdi V6) with a wavelength of $\lambda_{int} = 532$ nm and a 5 MHz linewidth is used to interrogate the resulting changes in optical properties of the investigated mixtures.

As depicted in Fig. 1 all beams are focused into the measurement volume. The generated spatially periodic perturbations scatter the interrogation beam. The resulting signal beam is filtered in space and spectrum using a laser-line filter, a coupler and single-mode fibres. An avalanche detector (Thorlabs APD110) is used for detection of the signal, which is logged with 20 GS/s by a 2.5 GHz bandwidth digital oscilloscope (LeCroy, WavePRO 254HD).

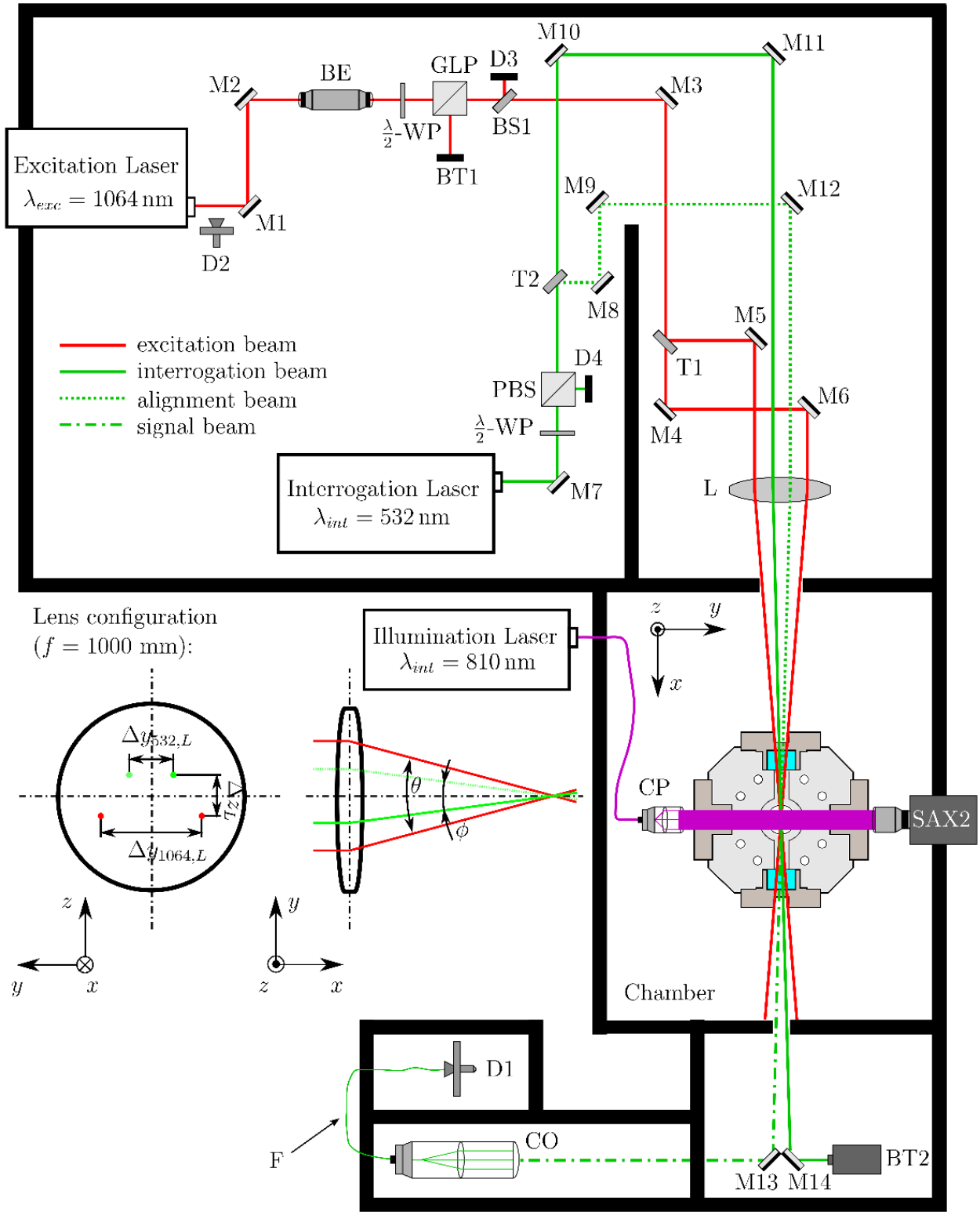

Fig. 1 Optical setup of the LITA system. BE: beam expander; BS: beam sampler; BT: beam trap; CP: coupler; CO: Collimator; D: detector (D1: Avalanche detector; D2: photo diode; D3, D4: thermal sensor); F: fibre; GLP: Glan–Laser polarizer; L: lens; M: mirror; PBS: polarised beam splitter; SAX2: high-speed camera (Photron FASTCAM SA-X2); T: beam splitter; WP: wave plate.

For the visualisation of the droplet evaporation process a shadowgraphy setup is utilised. The collimated light beam is generated by a fibre coupled laser (Cavitar Cavilux HF) with a wavelength of $\lambda_{exc} = 810$ nm, an operating frequency of 10 kHz and a laser pulse length of $\tau = 30$ ns. The shadowgram is spectrally filtered by a laser line filter (Edmund Optics) and captured with 10 kfps by a long-distance microscope (Infinity K2 DistaMax) and a high-speed camera (Photron FASTCAM SA-X2). Optical calibration yields 36 µm/px and a field of view of 33 x 8 mm. Note that the laser pulses of both the LITA and shadowgraphy setup are synchronised and lie within the exposure time of the high-speed camera.

4. Experimental setup

Transient investigations are performed in a temperature and pressure-controlled chamber designed for statistical investigations of evaporating free falling droplets in a near-critical environment. On top of the measurement chamber an independently temperature-controlled droplet generator is used for fluid injection. The chamber is operated as a homogeneous flow reactor with a constant gaseous and fluid mass flow. A description of the measurement chamber can be found in (Steinhausen, et al., 2021). The specification of the droplet generator can be found in (Lamanna, et al., 2020).

5. Signal processing

Applying curve fitting algorithms and direct Fourier analysis to extract macroscopic fluid properties, such as the speed of sound, require signals with a low signal to noise ratio in both the temporal as well as in the Fourier space. To ensure the necessary signal quality the LITA signals are filtered in both the temporal and frequency domain. First, all signals with a low signal intensity and all oversaturated signals are sorted out. Second, all signals are filtered based on the optimal shape of a non-resonant or resonant LITA signal in the frequency domain. For non-resonant signals the Fourier analysis leads to a single distinct non-zero frequency, whereas resonant signals show two distinct non-zero frequencies. The remaining valid signals are then averaged to calculate a mean LITA signal, which is used for curve fitting. An average LITA signal detected in the wake of an evaporating acetone droplet is exemplary depicted in Fig. 2. The signal is averaged using 4 valid LITA signals.

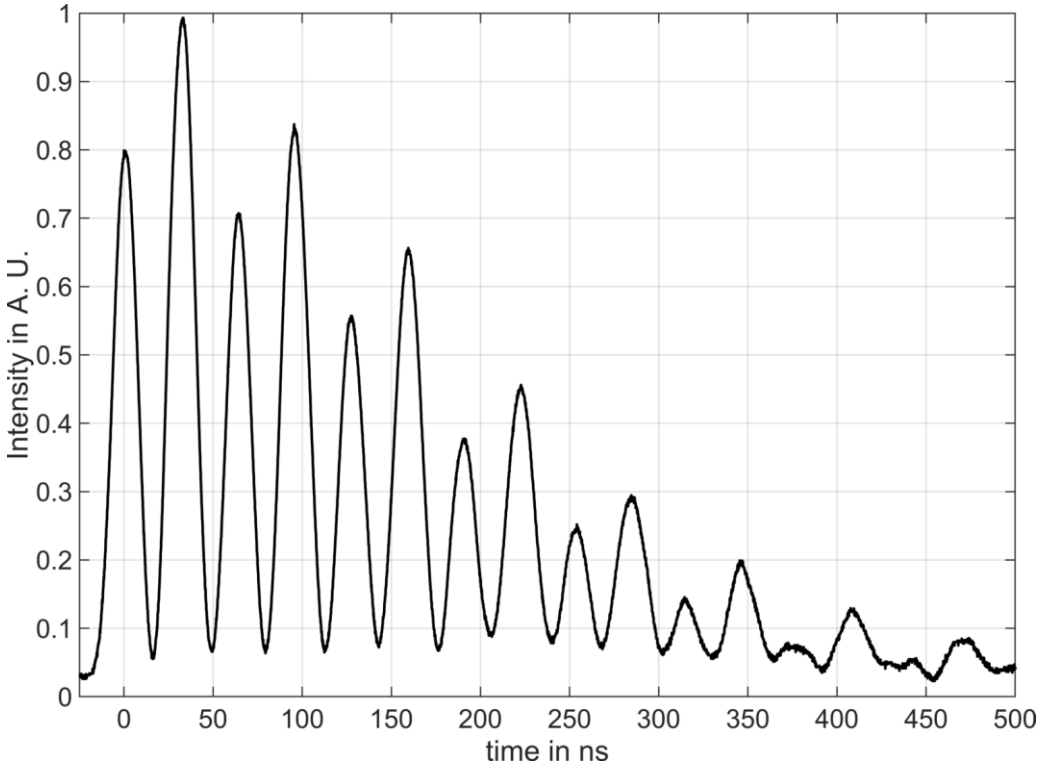

Fig. 2 Mean LITA signal at $t = 0.006$ s detected in a wake of an evaporating acetone droplet in a nitrogen atmosphere. Data is averaged over 4 valid signals and shows resonant fluid behaviour. $T_{\mathrm{r,Drop}} = 0.89$; $T_{\mathrm{r,ch}} = 1.01$; $p_{\mathrm{r,ch}} = 1.28$.

The resonant fluid behaviour shown by the signal is most likely a result of residual moisture in the acetone supply. Due to the absorption cross-section of water at the excitation wavelength, traces of solute water in acetone lead to a resonant fluid response, as has been previously discussed for carbon dioxide by (Steinhausen, et al., 2021). Besides good signal quality, the modelling of LITA signals requires deep understanding of the phonon-photon interaction inherent to the LITA measurement technique. Interaction of the density gradients in the droplets wake with the LITA wave packets can lead to distortion of the detected signal. This highlights the importance of the used signal filtering. Since equation (2) is highly dependent on the magnitude of the wave vector q and therefore on the grid spacing of the optical grid Λ, a thorough calibration is necessary. A detailed description of our calibration methodology as well as its validation is given in (Steinhausen, et al., 2021).

6. Results

Figure 3 depicts a sequence of shadowgrams for an evaporating free falling acetone droplet in a nitrogen atmosphere at different time steps. The atmospheric pressure is $p_{\mathrm{ch}} = 6$ MPa at a

temperature of $T_{\mathrm{N2}} = 513$ K. The droplet is preheated to a temperature of $T_{\mathrm{Drop}} = 453$ K. With respect to the critical values of acetone ($T_c = 508.1$ K, $p_c = 4.7$ MPa) this leads to the reduced operating conditions: $T_{\mathrm{r,Drop}} = 0.89$; $T_{\mathrm{r,ch}} = 1.01$; $p_{\mathrm{r,ch}} = 1.28$.

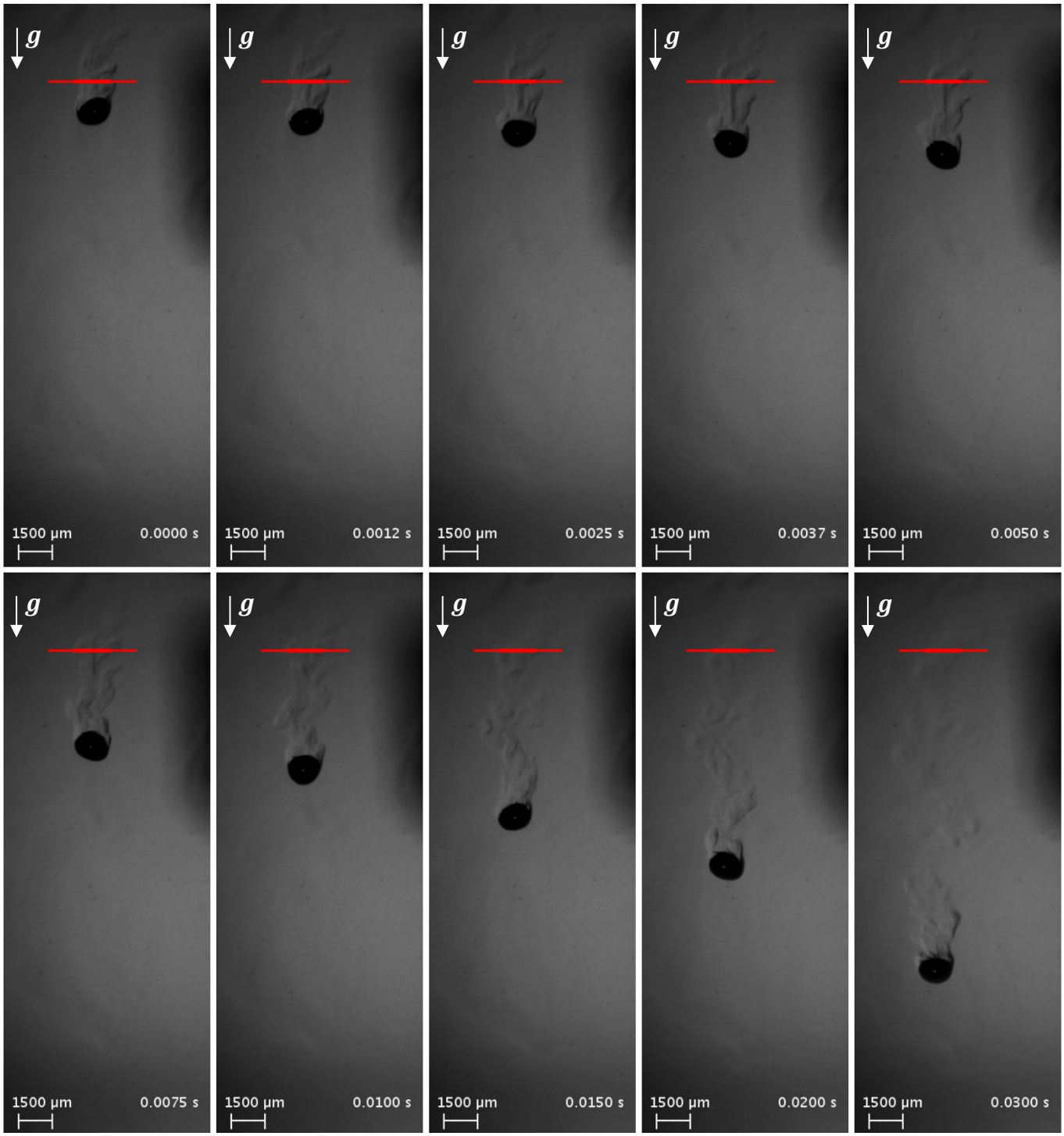

Fig. 3 Shadowgrams of the free-falling evaporating droplet. The position and size of the LITA measurement volume is indicated in red. The time stamp on the right lower corner is the time, synchronised with the time of the LITA data in Fig. 4. Droplet diameter is approximately $d_D = 1.3$ mm. $T_{\mathrm{r,Drop}} = 0.89$; $T_{\mathrm{r,ch}} = 1.01$; $p_{\mathrm{r,ch}} = 1.28$.

As is indicated by the ligaments in the wake of the droplet, evaporation is taking place. Unfortunately, our optical resolution is not high enough to detect changes in the droplet diameter due to evaporation, leading to a nearly constant equivalent diameter of approximately $d_D = 1.3$ mm. This observation is consistent with investigations by (Weckenmann, et al., 2014) under similar conditions. Due to the applied shadowgraphy technique, we are able to visualise changes in density gradients in the wake of the droplet. At the positon of the LITA measurement volume, which is indicated in red, stronger changes in the density gradient are observed for time steps below $t = 0.0075$ s. After $t = 0.0075$ s (lower row in Fig. 3) the shadowgrams indicate a similar behaviour over time at the LITA measurement position.

The speed of sound measurements in the droplets wake, shown in Fig. 4, support this observation. Note that the time stamp on the right lower corner in Fig. 3 is synchronised with the time of the speed of sound data in Fig. 4

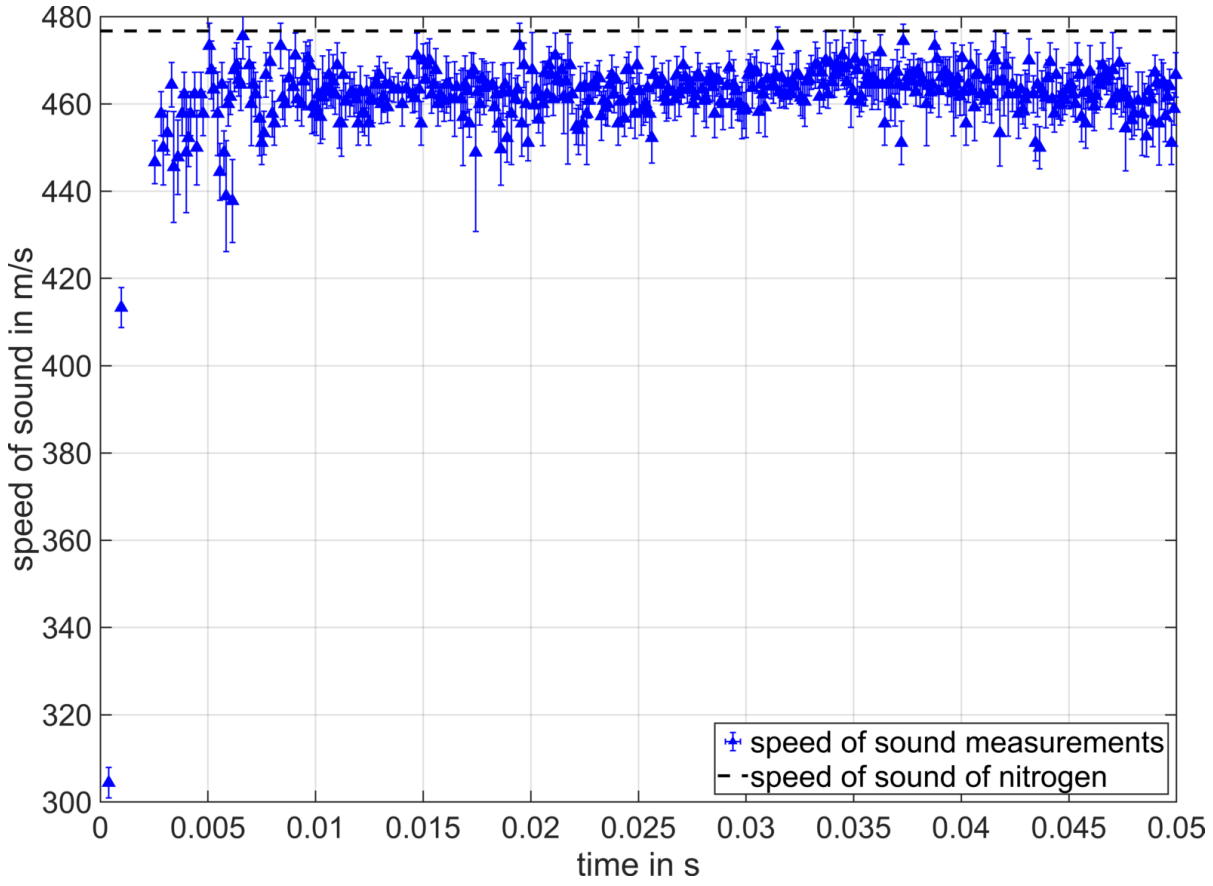

Fig. 4 Transient speed of sound measurements in a wake of an evaporated acetone droplet in a nitrogen atmosphere. Data is computed using equation (1). Droplet diameter is approximately $d_D = 1.3$ mm. $T_{\mathrm{r,Drop}} = 0.89$; $T_{\mathrm{r,ch}} = 1.01$; $p_{\mathrm{r,ch}} = 1.28$.

At early time steps the detected speed of sound is significantly lower as the speed of sound of nitrogen at measurement conditions. The speed of sound rises asymptotically with time until at $t = 0.0075$ s a more or less constant value slightly below the speed of sound of nitrogen is reached. This asymptotic behaviour in speed of sound is consistent with the shadowgraphy observations, which suggest a similar mixing process at time steps above $t \geq 0.0075$ s.

The explanation of the speed of sound measurements is twofold. First, we have to consider the speed of sound of a binary gaseous acetone-nitrogen mixture. For rising acetone concentrations, the mixtures speed of sound is decreasing, referred by (Lemmon, et al., 2018). Second, the speed of sound is increases with rising temperature. Hence, a lower temperature in the wake, due to evaporative cooling of the droplet, results in lower speed of sound in vicinity of the droplet. The temperature and concentration field in the droplet wake previously investigated by (Bork, et al., 2017) and (Preusche, et al., 2020) support these LITA observations.

In a next step an adiabatic mixing assumption can be applied to the speed of sound data. Since the speed of sound depends on concentration and temperature and both of these properties are connected by the adiabatic mixing assumption (see equation (5)), we can extract the temporal evolution of the concentration as well as the temperature in the droplets wake. By comparing this data to the concentration and temperature investigations previously performed by our research group, referred by (Bork, et al., 2017) and (Preusche, et al., 2020), we are able to validate the measurements against each other.

7. Conclusions

A transient LITA study in the wake of a free-falling evaporating droplet at near-critical conditions has been conducted. To the authors' best knowledge this is the first-time transient LITA measurements investigating macroscopic fluid phenomena, such as fluid injection processes, have been conducted. The droplet evaporation was hereby simultaneously visualised using shadowgraphy, whereas the speed of sound was directly detected by LITA at one location in the droplet wake. The results indicate a high acetone concentration at temperatures below the operating conditions in the droplets wake in direct vicinity of the droplet. These results are in general agreement with previous concentration and temperature investigation done by the authors. Based on the results, we conclude the feasibility of time resolved LITA measurements in macroscopic fluid phenomena.

Acknowledgements

The authors gratefully acknowledge the financial support by the Deutsche Forschungsgemeinschaft (DFG, German Research Foundation) – Project SFB-TRR 75, Project number: 84292822.

References

Baab, S., Förster, F. J., Lamanna, G., & Weigand, B. (2016). Speed of sound measurements and mixing characterization of underexpanded fuel jets with supercritical reservoir condition using laser-induced thermal acoustics. *Experiments in Fluids, 11*(57), 3068.

Baab, S., Steinhausen, C., Lamanna, G., Weigand, B., & Förster, F. J. (2018). A quantitative speed of sound database for multi-component jet mixing at high pressure. *Fuel*(233), 918-925.

Bork, B., Preusche, A., Weckenmann, F., Lamanna, G., & Dreizler, A. (2017). Measurement of species concentration and estimation of temperature in the wake of evaporating n-heptane droplets at trans-critical conditions. *Proceedings of the Combustion Institute, 2*(36), 2433–2440.

Crua, C., Manin, J., & Pickett, L. M. (2017). On the transcritical mixing of fuels at diesel engine conditions. *Fuel*(208), 535-548.

Cummings, E. B., Leyva, I. A., & Hornung, H. G. (1995). Laser-induced thermal acoustics (LITA) signals from finite beams. *Applied Optics, 18*(34), 3290–3302.

Falgout, Z., Rahm, M., Sedarsky, D., & Linne, M. (2016). Gas/fuel jet interfaces under high pressures and temperatures. *Fuel*(168), 14-21.

Förster, F. J., Crua, C., Davy, M., & Ewart, P. (2017). Time-resolved gas thermometry by laser-induced grating spectroscopy with a high-repetition rate laser system. *Experiments in Fluids, 7*(58), 1-8.

Gerber, V., Baab, S., Förster, F. J., Mandler, H., Weigand, B., & Lamanna, G. (2021). Fluid injection with supercritical reservoir conditions: Overview on morphology and mixing. *The Journal of Supercritical Fluids*(169), 105097.

Hemmerling, B., & Kozlov, D. N. (1999). Generation and temporally resolved detection of laser-induced gratings by a single, pulsed Nd:YAG laser. *Applied Optics, 6*(38), 1001.

Lamanna, G., Steinhausen, C., Weckenmann, F., Weigand, B., Bork, B., Preusche, A., . . . Gross, J. (2020). Laboratory experiments of high-pressure fluid drops. In *High-Pressure Flows for Propulsion Applications* (S. 49–109). American Institute of Aeronautics and Astronautics.

Lamanna, G., Steinhausen, C., Weigand, B., Preusche, A., Bork, B., Dreizler, A., . . . Gross, J. (2018). On the importance of non-equilibrium models for describing the coupling of heat and mass transfer at high pressure. *International Communications in Heat and Mass Transfer*(98), 49-58.

Lemmon, E. W., Bell, I. H., Huber, M. L., & McLinden, M. O. (2018). NIST standard reference database 23: Reference fluid thermodynamic and transport properties-REFPROP, Version 10.0, National Institute of Standards and Technology.

Müller, H., Niedermeier, C. A., Matheis, J., Pfitzner, M., & Hickel, S. (2016). Large-eddy simulation of nitrogen injection at trans- and supercritical conditions. *Physics of Fluids, 1*(28), 015102.

Preusche, A., Dreizler, A., Steinhausen, C., Lamanna, G., & Stierle, R. (2020). Non-invasive, spatially averaged temperature measurements of falling acetone droplets in nitrogen atmosphere at elevated pressures and temperatures. *The Journal of Supercritical Fluids*(166), 105025.

Schlamp, S., Cummings, E. B., & Hornung, H. G. (1999). Beam misalignments and fluid velocities in laser-induced thermal acoustics. *Applied Optics, 27*(38), 5724–5733.

Stampanoni-Panariello, A., Kozlov, D. N., Radi, P. P., & Hemmerling, B. (2005). Gas-phase diagnostics by laser-induced gratings II. Experiments. *Applied Physics B, 1*(81), 113–129.

Steinhausen, C., Gerber, V., Preusche, A., Weigand, B., A., D., & G., L. (2021). On the potential and challenges of laser-induced thermal acoustics for experimental investigation of macroscopic fluid phenomena. *Experiments in Fluids, 2*(62), 1-16.

Steinhausen, C., Lamanna, G., Weigand, B., Stierle, R., Gross, J., Preusche, A., . . . Sierra-Pallares, J. (2019). On the influence of evaporation on the mixture formation of high pressure combustion. *10th International Conference on Multiphase Flow, May 19 – 24, 2019.* Rio de Janeiro, Brazil.

Still, T. (2009). *High frequency acoustics in colloid-based meso- and nanostructures by spontaneous Brillouin light scattering.* Mainz, Germany: Ph.D.-Thesis, Johannes Gutenberg University Mainz.

Weckenmann, F., Lamanna, G., Weigand, B., Bork, B., & Dreizler, A. (2014). Experimental investigation of droplet injections in the vicinity of the critical point. *Proceedings 14th European Meeting on Supercritical Fluids: 18-21 May 2014.* Marseille, France.

Willman, C., Le Page, L. M., Ewart, P., & Williams, B. A. (2021). Pressure measurement in gas flows using laser-induced grating lifetime. *Applied Optics, 15*(60), C131-C141.